AD-A206 737

SECURITY CLASSIFICATION OF THIS PAGE *(When Data Entered)*

REPORT DOCUMENTATION PAGE

READ INSTRUCTIONS BEFORE COMPLETING FORM

1. REPORT NUMBER: AFOSR-TR- 89-0430
2. GOVT ACCESSION NO.
3. RECIPIENT'S CATALOG NUMBER

4. TITLE *(and Subtitle)*: Neural Network Models of Vector Coding, Learning, and Trajectory Formation during Planned and Reactive Arm and Eye Movements

5. TYPE OF REPORT & PERIOD COVERED: Interim report

6. PERFORMING ORG. REPORT NUMBER

AUTHOR(s): Stephen Grossberg

8. CONTRACT OR GRANT NUMBER(s): AFOSR F 49620-86-C-0037
AFOSR F 49620-87-C-0018

PERFORMING ORGANIZATION NAME AND ADDRESS

Center for Adaptive Systems
Department of Mathematics, Boston University
Boston, MA 02215

10. PROGRAM ELEMENT, PROJECT, TASK AREA & WORK UNIT NUMBERS: 61102F
21313/A5
2313 A5

CONTROLLING OFFICE NAME AND ADDRESS

AFOSR Life Sciences Directorate
Bolling Air Force Base
Washington, DC 20332

12. REPORT DATE: February 1989

13. NUMBER OF PAGES: 34

MONITORING AGENCY NAME & ADDRESS *(if different from Controlling Office)*

Same as 11

15. SECURITY CLASS. *(of this report)*: Unclassified

15a. DECLASSIFICATION/DOWNGRADING SCHEDULE

16. DISTRIBUTION STATEMENT *(of this Report)*

DISTRIBUTION STATEMENT A
Approved for public release;
Distribution Unlimited

17. DISTRIBUTION STATEMENT *(of the abstract entered in Block 20, if different from Report)*

18. SUPPLEMENTARY NOTES

To appear in Neural Programming, M. Ito (Editor), Proceedings of the Twelfth International Symposium of the Taniguchi Foundation, November 21-24, 1988, Lake Biwa, Japan.

19. KEY WORDS *(Continue on reverse side if necessary and identify by block number)*

Neural Networks; Eye Movement; Arm Movement; Robotics; Self-Organization, Learning; Trajectory Formation; Planning; Vector Coding.

20. ABSTRACT *(Continue on reverse side if necessary and identify by block number)*

Keywords

DD FORM 1 JAN 73 1473 EDITION OF 1 NOV 65 IS OBSOLETE

AIR FORCE OFFICE OF SCIENTIFIC RESEARCH (AFSC)
NOTICE OF TRANSMITTAL TO DTIC
This technical report has been reviewed and is approved for public release IAW AFR 190-12.
Distribution is unlimited.
MATTHEW J. KERPER
Chief, Technical Information Division

NEURAL NETWORK MODELS OF VECTOR CODING, LEARNING, AND TRAJECTORY FORMATION DURING PLANNED AND REACTIVE ARM AND EYE MOVEMENTS

Stephen Grossberg†
Center for Adaptive Systems
Boston University
111 Cummington Street
Boston, MA 02215 USA

To appear in **Neural Programming**, M. Ito (Editor)
Proceedings of the Twelfth International Symposium of the
Taniguchi Foundation, November 21–24, 1988, Lake Biwa, Japan

† Supported in part by the Air Force Office of Scientific Research (AFOSR F49620-86-C-0037 and AFOSR F49620-87-C-0018) and the National Science Foundation (NSF IRI-87-16960).

Acknowledgements: The author wishes to thank Cynthia Suchta and Carol Yanakakis for their valuable assistance in the preparation of the manuscript and illustrations.

1. Comparative Analysis of Movement Vectors in Eye and Arm Movements

Contemporary neural network models provide insights into some of the organizational principles that govern biological sensory-motor systems, and offer a level of computational precision that enables sharp comparisons and contrasts to be made between different sensory-motor systems. The capacity of these models to clarify, integrate, and predict behavioral and neural data is predicated upon the coordinated use of theoretical, mathematical, computational and empirical tools in a manner that reveals many more constraints on brain design than empirical tools alone. No single experimental paradigm in the behavioral and brain sciences provides sufficiently many data to uniquely characterize a neural system. Interdisciplinary theoretical and empirical approaches that can coordinate and discover both top-down and bottom-up constraints at multiple levels of behavioral and neural organization provide a much greater level of guidance towards characterizing brain designs.

The present chapter takes as its point of departure one important design principle that has been clarified by such an interdisciplinary approach. This is the principle of vector encoding that has been described, for example, in both the control of saccadic eye movements by the superior colliculus [40, 41, 46, 47, 48, 49] and the control of arm movements by the motor cortex [11, 15, 16, 17, 18, 20, 50].

Although neural vectors are encoded in both of these systems, they are encoded differently in each system. Why do both systems employ a neural code which, in its broad outline, seems similar, but in its computational realization is grossly different? Models of saccadic eye movements [28, 29] and of arm movements [3, 4, 5] have been developed in which these distinct types of vector coding are utilized. The models suggest that the design constraints which force these differences concern different problems of learning and coordinate transformation that are solved by the eye and arm movement systems. These design constraints are not, however, immediately evident in the neurophysiological experiments that discovered the vector codes. This chapter reviews and compares these constraints,

and suggests experiments that may be used to further test the models.

2. Map Vectors and Difference Vectors

The experiments of Sparks and his colleagues on the deeper layers of monkey superior colliculus have revealed a type of vector coding that may conveniently be called a *vector map code* [47]. In such a vector representation, each location in a spatially organized map encodes a different vector, hence, a different combination of movement length and direction. The most eccentric locations tend to code the longest movements. Changing the polar angle of a location tends to change movement direction. Exciting cells at a prescribed location in the map tends to cause a saccadic eye movement of corresponding length and direction. Populations of cells are activated under normal behavioral conditions. The eye movement triggered by such a population has a length and direction that corresponds to the average length and direction coded by all of the cells in the population.

The experiments of Georgopoulos and his colleagues on monkey motor cortex have revealed a type of vector encoding that may conveniently be called a *vector difference code* [16]. In such a vector representation, each cell tends to generate a broad unimodal tuning curve of direction preference that may include 180° of movement directions. Coding of movement amplitude tends to covary with the firing rate of cells in their direction of maximal sensitivity. Moreover, changes in the initial position of the arm covary with changes in the baseline level of cell activity. Thus a vector difference code does not encode amplitude and direction via different locations in a spatial map.

I now summarize models of eye and arm movement control in which the computation and design significance of these map vectors and difference vectors are clarified from the viewpoint of the system's total behavioral competence.

3. Vector Integration to Endpoint and GO Signal Modulation in Arm Movement Control

Difference vectors are found in a model of arm trajectory control, called the Vector Integration to Endpoint (VITE) model, that was developed by Bullock and Grossberg [3, 4, 5]. This model predicts how read-out of a target position command, or TPC, that specifies a desired target position, or motor expectation, is translated into a present position command, or PPC, that causes a synergy of arm muscles to contract and relax synchronously until the PPC equals the TPC. Figure 1 depicts the main variables that are computed by the VITE circuit.

Figure 1

Before describing these variables, it should be emphasized that such a command circuit forms only one part of the total neural system needed to control arm movements. For example, mechanisms for interaction of commands to opponent and synergetic muscles [3], for planning and timing the sequential readout of TPCs from working memory [28, 29 (chapter 9)], for adaptively linearizing and compensating for the variable gain of a nonlinear muscle plant [28, 29 (chapter 5)], and for adapting to the inertial properties generated by variable loads and velocities [6, 7] also form essential parts of the system for arm movement control.

Figure 1 shows that a TPC is subtracted from a PPC at a network stage at which a difference vector (DV) is computed. Model DV properties are remarkably similar to data properties reported by Georgopoulos and his colleagues (Figure 2). In particular, a large DV may be active without causing an overt movement. Such DV activation, called *motor priming*, has been reported by Georgopoulos, Schwartz, and Kettner [20]. The next stage of the model (Figure 1) computes the product of a DV and a GO signal, or gain control signal, that controls read-out of the movement command. The product DV $\times$ GO is integrated through time by the subsequent PPC stage. Due to this circuit design, the

PPC stage generates a continuous trajectory of synchronous outflow movement commands that gradually causes the PPC to approach the TPC at a speed that is regulated by the amplitude of the GO signal.

Figure 2

A large body of behavioral and neural data about arm and speech articulator movements has quantitatively been analysed by comparison with emergent properties of the VITE model. Here I summarize some neural data that support the existence of a GO signal, some predictions to further test the circuit's overall design, and a learning problem from which the circuit was derived.

4. GO Signal Generator in Globus Pallidus

Additional physiological support for the VITE model comes from recent experiments involving lesions and electrical stimulation of the basal ganglia. Data from a set of experiments by Horak and Anderson [32, 33] are consistent with the interpretation that the internal segment of the globus pallidus is an *in vivo* analogue of the VITE model's GO-signal generator.

An *in vivo* candidate for a GO-signal generator must pass three tests. First, stimulation at some site in the proposed pathway must have an effect on the *rate* of muscle contractions. Second, it must have this effect without affecting the *amplitude* of the contractions. Thus stimulation should have no effect on movement accuracy. Third, this rate-modulating effect should be *nonspecific*: it should affect all muscles that are typically synergists for the movement in question.

The studies conducted by Horak and Anderson [32, 33] addressed these issues. Horak and Anderson [32] showed that "when neurons in the globus pallidus were destroyed by injections of kainic acid (KA) during task execution, contralateral arm movement times (MT) were increased significantly, with little or no change in reaction times (p.290)." This satisfies the rate criterion. Moreover, the rate of motor recruitment was depressed "in

all the contralateral muscles studied at the wrist, elbow, shoulder, and back, but there were no changes in the sequential activation of the muscles (p.20)." This satisfies the non-specificity criterion. Finally, the authors also noted that "animals displayed no obvious difficulty in aiming accurately ... they did not miss the 1.5-cm target more often following KA injections, and there was no noticeable dysmetria around the target (p.300)." This satisfies the accuracy criterion.

Horak and Anderson [33] used an electrical stimulation paradigm instead of a lesion paradigm. They found that "stimulation in the ventrolateral internal segment of the globus pallidus (GP_i) or in the ansa lenticularis reduced movement time, whereas stimulation at many sites in the external pallidal segment (GP_e), dorsal (GP_i), and putamen increased movement times for the contralateral arm (p.305)." Once again, these effects were non-specific: "no somatotopic effects of stimulation were evident. If stimulation at a site produced slowing, it produced a depression of activity in all the muscles studied. Even stimulus currents as low as 25 μA affected proximal as well as distal muscles, flexor as well as extensor muscles, and early- as well as late-occurring activity (p.309)."

In the VITE model, activation of the GO-signal pathway produces movement only if instatement of a TPC different from the current PPC leads to the computation of a non-zero DV. In agreement with this property, Horak and Anderson [33] observed that "stimulation at sites that speeded movements did not induce involuntary muscle activation in resting animals nor did it change background EMG activity prior to self-generated activity during task performance (p.313)." In Bullock and Grossberg [3] it was noted that "very rapid freezing can be achieved by completely inhibiting the GO signal at any point in the trajectory". This property of the model has also been shown to be a property of the GP system. In particular, Horak and Anderson reported that "stimulation with 50 or 100 μA at ... sites ventral and medial to typical GP_i neuronal activity completely and immediately halted the monkey's performance in the task (p.315)." Taken together, their experiments led Horak and Anderson [33] to conclude that "the basal ganglia ... determine

the speed of the movement" (p.321).

5. Factorization of Position and Velocity Control

The striking correspondence between the experimental results of Georgopoulos *et al.* and of Horak and Anderson and the theoretical predictions of the VITE model regarding separate DV and GO-signal processes is important because it supports the hypothesis that motor systems, like sensory systems, implement a factorization of pattern and energy [24, 26, 27]. In the motor system, this factorization means that a movement's velocity ("energy") can be scaled up or down over a wide range without disrupting the movement's direction or terminal position ("pattern"). A similar hypothesis has recently been advanced by Eckmiller [9], who models it using a computationally different approach. Moreover, by using a GO-signal that grows gradually during the movement time, as in Figure 4, all synergists will complete their contractions at approximately the same time even if movement onset times of different synergists are staggered by a large amount [3]. These properties of the model, together with the growing evidence for separate DV and GO-signal pathways *in vivo*, provide a basis for understanding how primates can achieve space-time equifinality—all synergists reaching their length targets at equal times—yet retain separate control of velocity and position. Note that rate-control models relying on *static* stiffness adjustments (e.g., [8]) lack the critical temporal-equifinality property.

6. Amplification of Peak Velocity and a GO Signal Test

Several other important automatic compensatory properties emerge from interactions between the DV and GO processes. Bullock and Grossberg [3] noted that in addition to compensating for muscles that begin to contract at staggered onset times, the VITE circuit automatically compensates for changes of target position during the movement time. In particular, it was shown that the model generates the amplification of peak velocity that occurs during target-switching experiments [19]. Such a velocity amplification facilitates reaching the target after an incorrect initial TPC is replaced by an updated TPC.

This speed-up occurs "on-the-fly." It is not preprogrammed, but is rather an automatic emergent property of VITE circuit interactions. It is caused as follows.

First there is a rapid change in the TPC and thus in the DV. Then a more gradual change occurs in the DV and the PPC as the PPC integrates the DV through time. The velocity amplification is predicted to be caused by interaction of the new DV with the GO signal that was activated by the previous movement command. This prediction can be physiologically tested using an experiment that would also provide another opportunity to test if the Horak-Anderson cells in globus pallidus generate GO signals. Such a test would directly stimulate, at increasing levels of intensity, Horak-Anderson cells during a target switching task. Observed changes in movement velocity could then be used to calibrate the amount of change in GO signal amplitude caused by each level of stimulation.

7. Prediction and Test of Cells that Multiplex a Code for Local Velocity

The property of motor priming in motor cortex supports the VITE circuit prediction that there exists a stage subsequent to the DV stage at which an overt movement command is activated. The data of Horak and Anderson [32, 33] support the prediction that such activation may be partially controlled by a GO signal from the globus pallidus.

The VITE model may be further tested by recording from cells at the stage to which the motor cortex vector cells of Georgopoulos project. The cells at this subsequent stage should compute a measure of local movement velocity. This can be seen as follows.

These cells are predicted to compute (Figure 1) the product of rectified difference vector $[V]^+ = \max(V, 0)$ and GO signal G, namely

$$[V]^+ G. \tag{1}$$

The subsequent PPC stage computes a present position command P that performs a time integral of $[V]^+ G$, namely

$$P(t) = \int^t [V]^+ G dt. \tag{2}$$

Differentiating (2) shows that

$$\frac{dP}{dt} = [V]^+ G. \tag{3}$$

If subsequent network mechanisms cause the arm to follow closely the outflow movement command $P(t)$, then $\frac{dP}{dt}$ in (3) provides a good estimate of local movement velocity.

Equation (3) is of great interest from a conceptual point of view. It shows that the quantity $[V]^+ G$, which itself does not explicitly compute a velocity signal, *becomes* a velocity signal because of the manner in which it is transformed at subsequent network stages, in particular because it is integrated through time at the PPC stage.

The definition of this local velocity signal also depends upon the existence of a feedback loop between successive network stages (Figure 3). This feedback loop is needed to generate movements that are goal-oriented. This feedback loop is defined as follows. Quantity V in (3) computes a time-average of the difference between P and T, as in

$$\frac{d}{dt}V = \alpha(-V + T - P). \tag{4}$$

For simplicity, consider the case when the averaging rate α is large. Then, by (4),

$$V \cong T - P. \tag{5}$$

Hence, by (3) and (5),

$$\frac{d}{dt}P \cong [T - P]^+ G, \tag{6}$$

which summarizes the action of the feedback loop.

The approximate equation (6) shows that the local velocity signal is an emergent property of the entire network. It multiplexes quantities T, P, and G that are computed at three different network stages. It converts these quantities into a local velocity signal by using the feedback loop that exists between the DV stage and the PPC stage.

Given the motor cortical vector cells as an anatomical marker, it seems to be an experiment of great conceptual importance to test the existence of cells that code local

velocity at one of their target nuclei. If the stage coding local velocity is found, then a retrograde marker applied at this stage may identify a location in, or near, the global pallidus. Then a direct neurophysiological test of the existence of a GO signal may be made to supplement the data of Horak and Anderson [32, 33]. If globus pallidus cells are not marked, then this experiment may discover the true location of the GO signal generator. An anterograde marker applied at the local velocity stage may be used to discover the location of the PPC stage. Then a direct neurophysiological test can determine its ability to time-integrate local velocity signals.

8. Learning an Associate Map between Target Position Maps of the Eye-Head and Hand-Arm Movement Systems

Our theory suggests that the VITE circuit plays two distinct roles. One role, reviewed above, concerns trajectory formation within a sensory-motor system. This role may be called *intramodal trajectory formation.* The second role concerns *intermodal learning of target position maps.* This latter role is schematized by Figure 3. The remarkable fact is that the same TPC, DV, and PPC stages are predicted to accomplish both roles.

Figure 3

The learning process transforms stored representations of a target position coded with respect to the eye-head system into a target position command of the hand-arm system for moving the arm, via VITE dynamics, to that position in space.

This mapping process is of critical importance in sensory-motor control because many arm movements are activated in response to visually seen objects that the individual wishes to grasp. This transformation must be learned because, as the arm grows, the motor commands which move it to a fixed position in space with respect to the body must also change in an adaptive fashion. Our central problem is thus formulated as follows: How is a transformation learned and adaptively modified between the parameters of the eye-head system and the hand-arm system so that an observer can touch a visually fixated object?

Following Piaget's [44] analysis of *circular reactions*, imagine that an infant's hand makes a series of unconditional movements, which the infant's eyes unconditionally follow. As the hand occupies a variety of positions that the eye fixates, a transformation is learned from the parameters of the hand-arm system to the parameters of the eye-head system. A reverse transformation is also learned from parameters of the eye-head system to parameters of the hand-arm system. This reverse transformation enables an observer to intentionally move its hand to a visually fixated position.

Not all positions that the eye-head system or the hand-arm system assume are the correct positions to associate through learning. For example, suppose that the hand briefly remains at a given position and that the eye moves to foveate the hand. An infinite number of positions are assumed by the eye as it moves to foveate the hand. Only the final, intended, or expected position of the eye-head system is a correct position to associate with the position of the hand-arm system.

Learning of an intermodal motor map must thus be prevented except when the eye-head system and the hand-arm system are near their intended positions. Otherwise, all possible positions of the two systems could be associated with each other, which would lead to behaviorally chaotic consequences. Several important conclusions follow from this observation [3, 26, 28]:

(1) All such adaptive sensory-motor systems compute a representation of target position. This representation is the TPC.

(2) All such adaptive sensory-motor systems also compute a representation of present position. This representation is the PPC.

(3) During movement, target position is matched against present position. Intermodal map learning is prevented except when target position approximately matches present position, that is, except when the DV is small (Figure 3). A *learning gate*, or modulator, signal is thus controlled by the DV. This gating signal enables learning to occur when a

good match occurs and prevents learning from occurring when a bad match occurs.

In summary, we trace the existence of vector difference codes to two fundamental computational problems: intermodal learning of target position transformations, and intramodal performance of synchronous trajectories within dynamically determined motor synergies.

9. Visually Reactive Movements and the Vector Map Code within Superior Colliculus

The type of vector map code described by Sparks and his colleagues may be analysed as part of a circuit design that realizes a different type of learning process. This learning process enables the *visually reactive movement system* to generate accurate reactive eye movements in response to flashing or moving lights on the retina [28, 29 (chapters 2, 3, and 11)]. The role of map vectors in the visually reactive movement system has been analysed as part of a developmental sequence during which reactive eye movements to flashing or moving lights on the retina are supplemented by attentionally mediated movements towards motivationally interesting sensory cues. These movements are supplemented once again by predictive eye movements that form part of planned sequences of complex movement synergies capable of ignoring the sensory substrate on which they are built. Each of these categories of eye movement requires one or more types of learning in order to achieve high accuracy. The movement systems wherein attention and intention play an increasingly important role base their adaptive success upon the prior learning of the more primitive, visually reactive types of movement.

10. Three Interacting Coordinate Systems: Retinotopic, Motor Sector, and Map Vector

The visually reactive movement system uses learning based upon visual error signals to improve the accuracy of its movements. It is assumed that a target light is chosen and stored in short term memory (STM) before a movement starts (Figure 4). This stored

representation activates a movement along an unconditioned movement pathway. The movement amplitude and direction, before learning, are controlled by a transformation of the retinal location of the stored representation into a motor representation in which the most eccentric positions generate the largest movement signals. This is accomplished by decomposing the motor representation into hemifields (Figure 5), and assuming that the gradient of connections to the corresponding pairs of agonist and antagonist muscles increases with eccentricity [10, 14, 21].

Figure 4

Figure 5

The target light is stored in STM so that it can benefit from a visual error signal after the movement terminates. The stored representation samples this visual error signal along a conditioned movement pathway (Figure 4) whose output summates with that of the unconditioned pathway to generate the total movement signal. Thus learning within this system controls a feedforward adaptive gain that is changed by visual error signals.

How these visual error signals are coded clarifies one aspect of why a vector map exists in the deeper layers of superior colliculus. As illustrated by Figure 4, each light plays two roles: it acts as a movement signal for the next movement, and an error signal for the last movement. Thus the retinal location of each light must be remapped into a type of motor coordinates that can correct the full range of typical movement errors. The theory suggests that this is accomplished as follows.

11. Automatic Gain Control of Movement Commands by Visual Error Signals: Cerebellar Learning

The theory predicts how each movement command pathway can individually benefit from visual error signals to generate a more accurate movement in the future. Its analysis leads to a model of learning by the cerebellum which extends earlier models of cerebellar learning [1, 2, 12, 13, 22, 23, 25, 34, 35, 39, 42]. I emphasize two key properties of this

model herein: (i) the dual action of each light; and (ii) the learning of a motor synergy. The previous section summarized the network anatomy that subserves the dual action property.

12. Learning a Motor Synergy: Opponent Processing of Error Signals

The second key property of the AG stage concerns its ability to convert visual error signals, which individually activate only a *single* retinal position, into correct and synchronous movement commands to *all* muscles which move the eye. Learning of a motor synergy takes place in the Adaptive Gain Stage, or AG stage (Figure 4). The AG stage is identified with the cerebellar vermis, based upon data which show that this brain region controls modification of a saccade's *pulse gain* [43]. The conditioned movement pathway generates sampling signals which pass through the AG stage and add or subtract a conditionable movement signal to the total movement command. An error signal acts to change the size, or gain, of the conditionable movement signal. Thus the AG stage is a region where automatic gain control of the total movement command takes place.

In order to learn a motor synergy, the system preprocesses the error signals before they can be sampled by the conditioned movement pathway. Two processing constraints conceptualize these preprocessing stages: (a) the Opponent Processing constraint, and (b) the Equal Access constraint. The need for Opponent Processing—which is a new feature of our model—can be seen as follows.

Each eye is moved by three pairs of agonist and antagonist muscles. One pair moves the eye horizontally. The other two pairs move the eye obliquely, and together can generate vertical movements. I now indicate why an *increase* in the gain of an agonist muscle command must generate a *decrease* in the gain of the corresponding antagonist muscle command, and conversely. In other words, each visual error signal has antagonistic, or opponent, effects on the conditionable gains of the muscle commands which it changes.

In order to realize the Opponent Processing constraint, suppose that the retina is to-

pographically transformed from retinotopic coordinates into a motor map containing six sectors (Figure 6a). This motor sector map is an idealization that may be compared to the data of Sparks and his colleagues. Each pair of agonist-antagonist muscles—(α^+, α^-), (β^+, β^-), (γ^+, γ^-)—is represented by opposite sectors in the sector map. A visual error signal which falls within a prescribed sector increases the conditioned gain of the corresponding muscle and decreases the conditioned gain of the antagonistic muscle. This type of retinal-to-motor transformation can be used to correct undershoot, overshoot, and skewed movement errors as follows.

Figure 6

Suppose that a light activates the retinal position labelled 1 in Figure 6b and thereby causes a saccade. Suppose that, after movement, the light activates position 2. Such a movement defines an undershoot error: the eye does not move far enough toward the right to foveate the light. If the error signal increases the gain of muscle β^+ and decreases the gain of muscle β^-, then the eye will move further toward the right the next time that position 1 is activated, thereby tending to correct the undershoot error.

The need for opponent processing can be seen by considering the case of an overshoot error in Figure 6c. Here a light to position 1 moves the eye in such a way that the error signal activates a position 2 on the opposite side of the fovea. In other words, the eye moves too far to the right. Due to opponent processing, the error signal increases the gain of muscle β^- and decreases the gain of muscle β^+, thereby tending to correct the overshoot error the next time position 1 is activated. A similar analysis shows how opponent processing of error signals corrects skewed errors, as in Figure 6d.

13. The Equal Access Constraint

Figure 6 emphasizes the fact that, before learning occurs, a light to a fixed retinal position (1) can cause undershoot, overshoot, or skewed errors. The system cannot *a priori* predict which type of error will occur as a result of its inadequately tuned parameters. In

order to correct any possible error, each position must be able to activate a conditioned movement pathway that is capable of sampling error signals delivered to *any* of the motor sectors. This is the Equal Access constraint, which was first articulated in a formal model of cerebellar learning by Grossberg [22, 23].

In order to realize the Equal Access constraint, we have assumed [28, 29 (chapter 3)] that the motor sectors are mapped, via a complex logarithmic map [45], into motor strips (Figure 7). Then a single conditioned movement pathway can sample gain changes due to error signals which activate any motor strip. Figure 8 describes two variants of this design. Each variant realizes both the Opponent Processing constraint and the Equal Access constraint. Fujita [14] has also used the complex log map in his work on saccadic eye movements.

Figure 7

Figure 8

The by now classical cerebellar interpretation of this anatomy is that the sampling signals are carried by parallel fibers through the dendrites of Purkinje cells, whereas the error signals are carried by climbing fibers to the Purkinje cell dendrites [1, 22, 23, 25, 34, 35, 39].

In summary, visual error signals are mapped from retinotopic coordinates into motor sector coordinates and then into motor strip coordinates, so that they can all be sampled by individual movement commands within pathways capable of reading-out the conditioned gain signals to the appropriate target muscles. Such a transformation provides a simple explanation of the type of vector map described by Sparks: An increase in map eccentricity increases movement length and a change in map polar angle changes movement direction because such a representation enables visual error signals to be mapped into motor commands that are capable of correcting undershoot, overshoot, and skewed errors in visually reactive movements.

14. The Vector-to-Sector Transform: Dimensional Consistency of Planned Vectors and Reactive Retinotopic Commands

It remains to discuss why the deeper layers of superior colliculus code movement *vectors*, rather than merely motorically transformed retinotopic commands. An analysis of this problem is spread over several chapters of Grossberg and Kuperstein [28, 29 (chapters 3, 4, 6, 10, 11)]. Here I outline some of the main design themes.

Perhaps the most salient issue concerns the apparent absurdity of using vector encoding when the problem is considered from a common-sense point of view. In order to compute a vector, the retinotopic location R of a light must be combined with the initial position E of the eye in the head to generate a target position T of the light in head coordinates. Let us symbolically represent this transformation by

$$T = R + E. \tag{7}$$

Then a vector V is computed by subtracting E from T:

$$V = T - E. \tag{8}$$

On the other hand, the eye moves in the head. Thus, all motor commands M must be recoded into head-coordinates again before activating the saccade generator that moves the eye:

$$M = V + E. \tag{9}$$

A comparison of equations (7)–(9) seems to suggest much ado about nothing, because (7) implies that

$$R = T - E, \tag{10}$$

so that M could have been derived directly from T without computing V at all!

The functional significance of these transformations is clarified by noting that vector coordinates V are consistent with retinotopic coordinates R, but head coordinates, T

and M, are not. Visual error signals within the visually reactive movement system are retinotopically coded before being remapped into a retinally consistent motor sector map. In order for head-centered, attentive, planned movement commands T to benefit from the movement accuracy that is learned using visual error signals, they must be transformed into a retinally consistent coordinate system. Comparison of (8) and (9) illustrates that movement vectors V (of the type studied by Georgopoulos!) are consistent with retinal and motor sector coordinates. Thus the head commands T are transformed into vectors V so that the vectors V can be transformed into a motor sector code. In this way, attentive, planned movements can achieve the learned accuracy of visually reactive movements. This vector-to-sector transformation converts the motor sector map into a vector map.

15. Movement Gating, Intermodal Mapping, and Competition between Planned and Reactive Movements

The vector-to-sector transform is a learned transformation. Our model of how this learning process occurs [28 (chapter 11)] clarifies how vectors V can learn to control the movement pathways activated by a retinal position R during visually reactive movements when the vector V is derived from R, and thus $V = R$. The model also predicts how, after learning is over, a visually reactive movement to position R can be suppressed via a spatially organized competitive interaction (cf. [14]) when an intended movement command V is activated such that $V \neq R$. Despite this suppression, the model explains how the movement controlled by V achieves the accuracy derived from the cerebellar gains learned by visually reactive error signals. The analysis also suggests how auditory signals [36, 37, 47] and planned movement sequences [38] can activate accurate saccadic eye movements, and how inhibitory gating of superior colliculus by substantia nigra enables planned attentive movement commands to successfully compete with more rapidly processed reactive movement commands [30, 31].

16. Summary

This chapter clarifies the functional role played by two types of vector codes—vector map codes and vector difference codes—in the control of saccadic eye movements by the superior colliculus and the control of planned arm movements by the motor cortex, respectively. Vector difference codes form part of a neural network model, called the Vector Integration to Endpoint (VITE) Model, that converts a target position command into a series of continuously integrated present position commands which are capable of generating a synchronous arm movement trajectory. The different vectors are converted into overt movement commands by a gain control signal, called the GO signal, whose generator may be in globus pallidus. Experiments concerning how to discover predicted cells coding local velocity, GO signal, and present position commands are suggested. The VITE circuit is also predicted to play a role in modulating the learning of transformations from parietal target position representations of the eye-head system to target position commands of the hand-arm system.

The vector map codes are suggested to arise due to the interaction of several subsystems of the saccadic eye movement system. A visually reactive movement system uses visual error signals to correct motor synergies that are activated by visual signals. To accomplish this visual-to-motor learning process, the visual error signals are recoded into a motor sector map. An analysis of how movement errors are corrected by this system suggests a refined model of cerebellar learning, notably learning in the cerebellar vermis.

In order for the planned and attentive saccadic eye movement subsystems to benefit from visually reactive learning, they code their movement commands into vectors which are dimensionally compatible with the motor sector code, and then transform the vectors into the motor sector code. This vector-to-sector transformation converts the motor sector code into the type of vector map found in the deeper layers of superior colliculus. The properties of this transformation clarify how auditory signals and planned, attentive movement sequences may benefit from learning within the visually reactive movement system,

and how gating of superior colliculus by substantia nigra enables the competition between these several movement systems to be successfully completed.

REFERENCES

1. Albus, J.S. (1971). *Math. Biosci.*, **10**, 25–61.

2. Brindley, G.S. (1964). *Intnl. Brain Res. Org. Bull.*, **3**, 80.

3. Bullock, D. and Grossberg, S. (1988a). *Psych. Rev.*, **95**, 49–90.

4. Bullock, D. and Grossberg, S. (1988b). In J. A. S. Kelso (Ed.), **Dynamic patterns in complex systems**. Hong Kong: World Scientific Publishers.

5. Bullock, D. and Grossberg, S. (1988c). In H. Haken (Ed.), **Neural and synergetic computers**. New York: Springer-Verlag, 197–228.

6. Bullock, D. and Grossberg, S. (1988d). *Neural Networks* (Supplement), **1**, 329.

7. Bullock, D. and Grossberg, S. (1989). Submitted for publication.

8. Cooke, J.D. (1980). In G. E. Stelmach and J. Requin (Eds.), **Tutorials in motor behavior**. Amsterdam: North-Holland, 199–212.

9. Eckmiller, R., this volume.

10. Edwards, S.B. (1980). In J. A. Hobson and M. A. Brazier (Eds.), **The reticular formation revisited: Specifying functions for a non-specific system**. New York: Raven Press, 193–209.

11. Evarts, E.V. and Tanji, J. (1974). *Brain Res.*, **71**, 479–494.

12. Fujita, M. (1982a). *Biol. Cybernetics*, **45**, 195–206.

13. Fujita, M. (1982b). *Biol. Cybernetics*, **45**, 207–214.

14. Fujita, M., this volume.

15. Georgopoulos, A.P. (1986). *Ann. Rev. Neurosci.*, **9**, 147–170.

16. Georgopoulos, A.P., this volume.

17. Georgopoulos, A.P., Kalaska, J.F., Caminiti, R., and Massey, J.T. (1982). *J. Neurosci.*, **2**, 1527–1537.

18. Georgopoulos, A.P., Kalaska, J.F., Crutcher, M.D., Caminiti, R., and Massey, J.T. (1984). In G. M. Edelman, W. E. Goll, and W. M. Cowan (Eds.), **Dynamic aspects of neocortical function**. Neurosciences Research Foundation, 501–524.

19. Georgopoulos, A.P., Kalaska, J.F., and Massey, J.T. (1981). *J. Neurophysiol.*, **46**, 725–743.

20. Georgopoulos, A.P., Schwartz, A.B., and Kettner, R.E. (1986). *Science*, **233**, 1416–1419.

21. Gisbergen, J.A.M. van, Robinson, D.A., and Gielen, S. (1981). *J. Neurophysiol.*, **45**, 417–442.

22. Grossberg, S. (1964). **The theory of embedding fields with applications to psychology and neurophysiology**. New York: Rockefeller Institute for Medical Research.

23. Grossberg, S. (1969). *Studies Appl. Math.*, **48**, 105–132.

24. Grossberg, S. (1970). *J. Theor. Biol.*, **27**, 291–337.

25. Grossberg, S. (1972). *Kybernetik*, **10**, 49–57.

26. Grossberg, S. (1978). In R. Rosen and F. Snell (Eds.), **Progress in theoretical biology**, Vol. 5. New York: Academic Press, 233–374.

27. Grossberg, S. (1982). **Studies of mind and brain: Neural principles of learning, perception, development, cognition, and motor control**. Boston: Reidel Press.

28. Grossberg, S. and Kuperstein, M. (1986). **Neural dynamics of adaptive sensory-motor control: Ballistic eye movements**. Amsterdam: Elsevier/North-Holland.

29. Grossberg, S. and Kuperstein, M. (1989). **Neural dynamics of sensory-motor control, Expanded Edition**. Elmsford, NY: Pergamon Press.

30. Hikosaka, O., this volume.

31. Hikosaka, O. and Wurtz, R.E. (1983). *J. Neurophysiol.*, **49**, 1268–1284.

32. Horak, F.B. and Anderson, M.E. (1984a). *J. Neurophysiol.*, **52**, 290–304.

33. Horak, F.B. and Anderson, M.E. (1984b). *J. Neurophysiol.*, **52**, 305–322.

34. Ito, M. (1974). In F. O. Schmidt and F. G. Worden (Eds.), **The neurosciences third study program**. Cambridge, MA: MIT Press.

35. Ito, M. (1984). **The cerebellum and neural control**. New York: Raven Press.

36. Knudsen, E.I. (1984). *Trends in Neurosci.*, **7**, 326–330.

37. Konishi, M. (1984). In L. Bolis, R. D. Keynes, and S. H. P. Maddrell (Eds.), **Comparative physiology of sensory systems**. Cambridge: Cambridge University Press.

38. Kowler, E. (1982). Characteristics and visual consequences of saccades used to scan displays. Presentation at AFOSR Technical Meeting, Sarasota, Florida.

39. Marr, D. (1969). *J. Physiol. (London)*, **202**, 437–470.

40. Mays, L.E. and Sparks, D.L. (1980). *Science*, **208**, 1163–1165.

41. Mays, L.E. and Sparks, D.L. (1981). In A. F. Fuchs and W. Becker (Eds.), **Progress in oculomotor research**. New York: Elsevier/North-Holland, 39–47.

42. McCormick, D.A. and Thompson, R.F. (1984). *Science*, **223**, 296–299.

43. Optican, L.M. and Robinson, D.A. (1980). *J. Neurophysiol.*, **44**, 1058–1076.

44. Piaget, J. (1963). **The origins of intelligence in children**. New York: Norton.

45. Schwartz, E.L. (1980). *Vision Res.*, **20**, 645–669.

46. Sparks, D.L. (1978). *Brain Res.*, **156**, 1–16.

47. Sparks, D.L., this volume.

48. Sparks, D.L. and Jay, M. (1987). In M. A. Arbib and A. R. Hanson (Eds.), **Vision, brain, and cooperative computation**. Cambridge, MA: MIT Press, 109–128.

49. Sparks, D.L. and Mays, L.E. (1981). In A. F. Fuchs and W. Becker (Eds.), **Progress in oculomotor research**. New York: Elsevier/North-Holland.

50. Tanji, J. and Evarts, E.V. (1976). *J. Neurophysiol.*, **39**, 1062–1068.

FIGURE CAPTIONS

Figure 1. Main variables of the VITE circuit: T = target position command, V = difference vector, G = GO signal, P = present position command. The circuit does not include the opponent interactions that exist between the VG and P stages of agonist and antagonist muscle commands.

Figure 2. Data and simulation of vector cell through time: (a) Quick buildup and gradual decline of activity in motor cortex vector cells. (Reprinted with permission from [19].) (b) Computer simulation of the model variables V, G, and P in response to a step increment in T. Note the similarity between the graph of V and the vector cell profile in (a). (Reprinted with permission from [3].)

Figure 3. Learning of intermodal transformation between target position representations is gated by the difference vector DV. This gate helps to prevent incorrect associations from being learned between eye-head TPCs and hand-arm TPCs during motor development. (Reprinted with permission from [3].)

Figure 4. A target light position is chosen for storage in short term memory (STM) before a movement. Its stored representation activates parallel movement command pathways. The unconditioned pathway generates a movement that may be inaccurate. The conditioned pathway reads-out an adaptive gain control signal whose size may be altered by learning. Learning occurs at an adaptive gain (AG) stage whose design is compared with cerebellar architecture. Learning is driven by a visual error signal that is activated, after the movement terminates, by the location of a newly chosen target light with respect to the fovea.

Figure 5. The retinotopically coded location of a stored target light is recoded into a motor map that is divided into hemifields. More eccentric locations in each hemifield

generate larger excitatory and inhibitory movement signals to the corresponding agonist and antagonist muscles, respectively. Opposite hemifields send opponent signals to each other's agonist muscles. When all three pairs of hemifield maps that move an eye are joined together, they give rise to a motor sector map (Figure 6).

Figure 6. Transformation of retinally registered visual movement commands into a motor sector map that can be used to correct visually reactive movement commands. (a) Retinal surface is transformed into motor sectors corresponding to agonist muscles $(\alpha^+, \beta^+, \gamma^+)$ and antagonist muscles $(\alpha^-, \beta^-, \gamma^-)$ of one eye. The text describes how the sectors convert retinotopic locations of visual movement signals and visual error signals into learned movement gain changes at the AG stage. In (b)–(d), number 1 designates the retinal position of the target light that is stored in STM and causes the movement. Number 2 designates the retinal position of the target light, after the movement terminates, that acts as an error signal. The motor sector map determines which muscle movement gains will be changed by the error signal. The sharp boundaries of the motor sector map are an idealization of partially overlapping motor sector regions. (b) A saccadic undershoot error. (c) An overshoot error. (d) A skewed undershoot error. (Reprinted with permission from [28].)

Figure 7. Logarithmic map from sensory sectors into motor strips: Each sensory hemifield $(\alpha^+, \beta^+, \gamma^+)$ and $(\alpha^-, \beta^-, \gamma^-)$ maps into a row of parallel motor strips. In this fractured somatotopy, the strips of agonist-antagonist pairs (α^+, α^-), (β^+, β^-), and (γ^+, γ^-) are juxtaposed, much as in the case of ocular dominance columns in the striate cortex. A pair of motor strip maps is depicted, one in each AG stage hemisphere. Outputs from all agonist-antagonist pairs compete before the net outputs perturb the saccade generator. This circuit works even if only agonist muscles $(\alpha^+, \beta^+, \gamma^+)$ receive excitatory error signals in one hemifield and antagonist muscles $(\alpha^-, \beta^-, \gamma^-)$ receive excitatory error signals in the other hemifield. An excitatory error signal to the α^+ strip can weaken the net α^- output of the contiguous strip via competition of the outputs, but cannot strengthen the

α^- output signal. An excitatory error signal to the α^- strip of the other hemifield can strengthen the net α^- output. (Reprinted with permission from [28].)

Figure 8. Two ways to achieve opponent conditioning of agonist-antagonist muscles: (a) An error signal increases the conditioned gain at the agonist muscle strip and decreases the conditioned gain at the antagonist muscle strip; (b) An error signal increases the conditioned gain at the agonist muscle strip. Competition between agonist and antagonist muscle strip outputs causes the decrease in the net antagonist output. (Reprinted with permission from [28].)

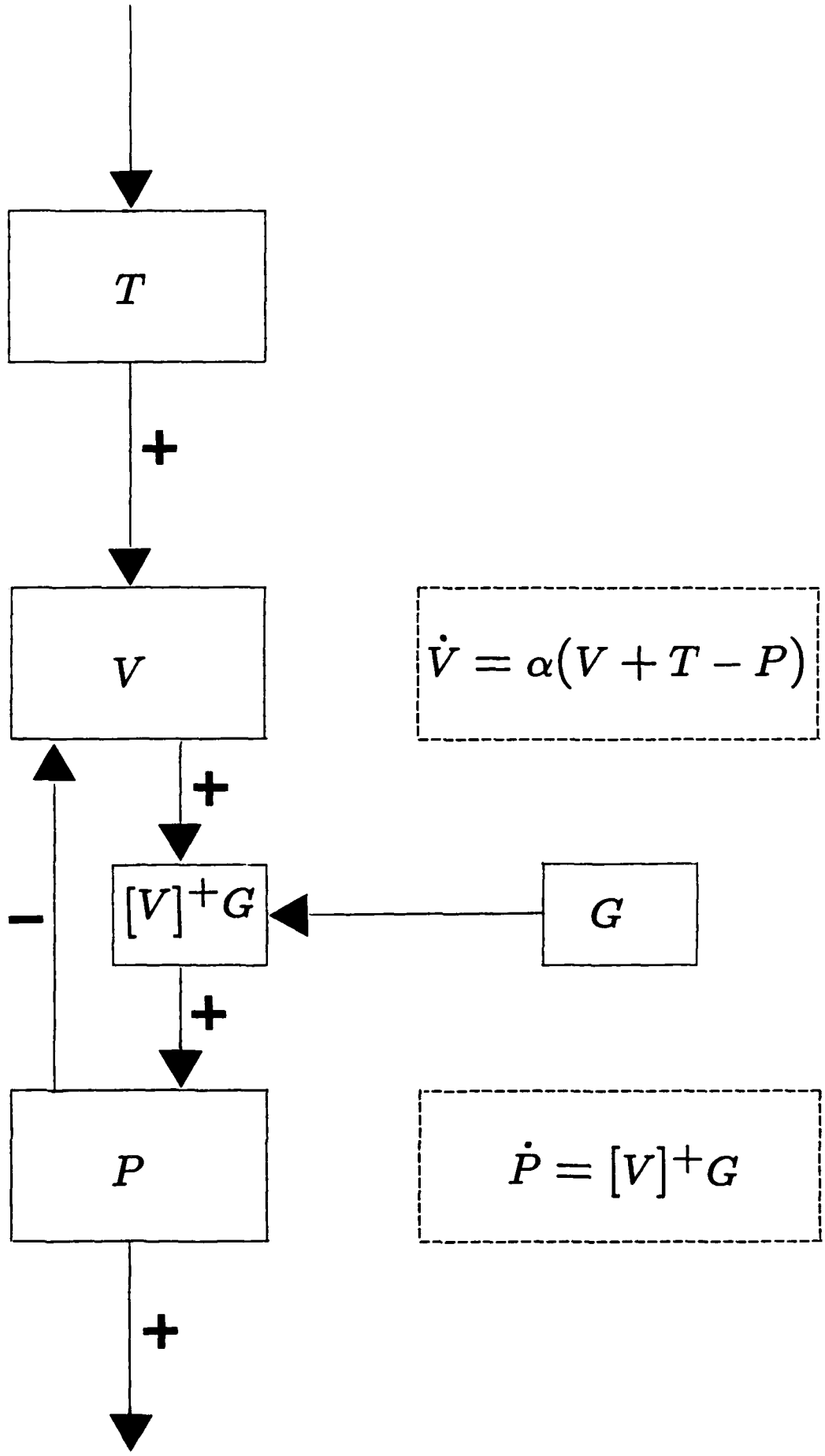

Figure 1

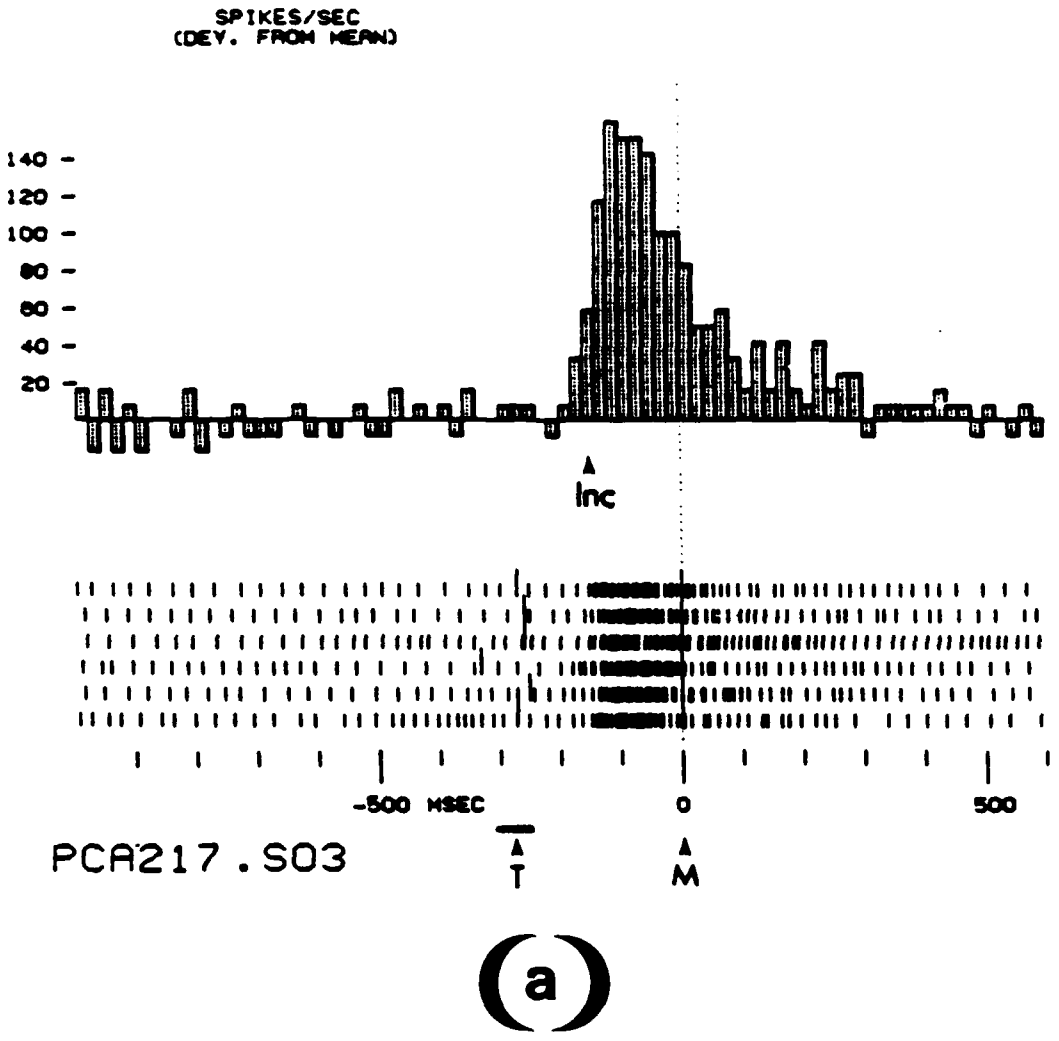
SPIKES/SEC
(DEV. FROM MEAN)
140
120
100
80
60
40
20
Inc
-500 MSEC
0
500
PCA217.S03
T
M

(a)

Figure 2a

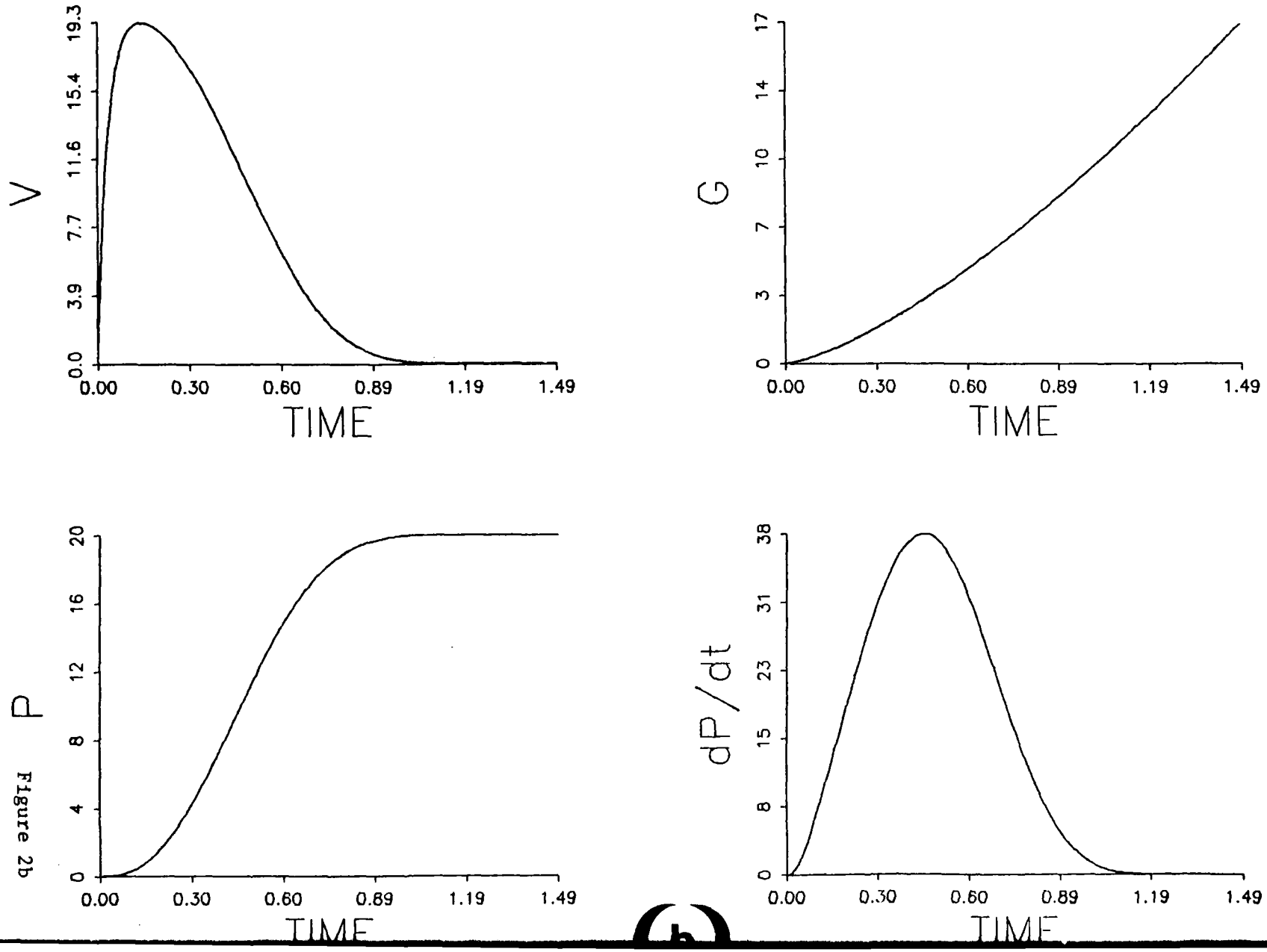
V
0.0
3.9
7.7
11.6
15.4
19.3
0.00
0.30
0.60
0.89
1.19
1.49
TIME
G
0
3
7
10
14
17
0.00
0.30
0.60
0.89
1.19
1.49
TIME
P
0
4
8
12
16
20
0.00
0.30
0.60
0.89
1.19
1.49
TIME
dP/dt
0
8
15
23
31
38
0.00
0.30
0.60
0.89
1.19
1.49
TIME

Figure 2b

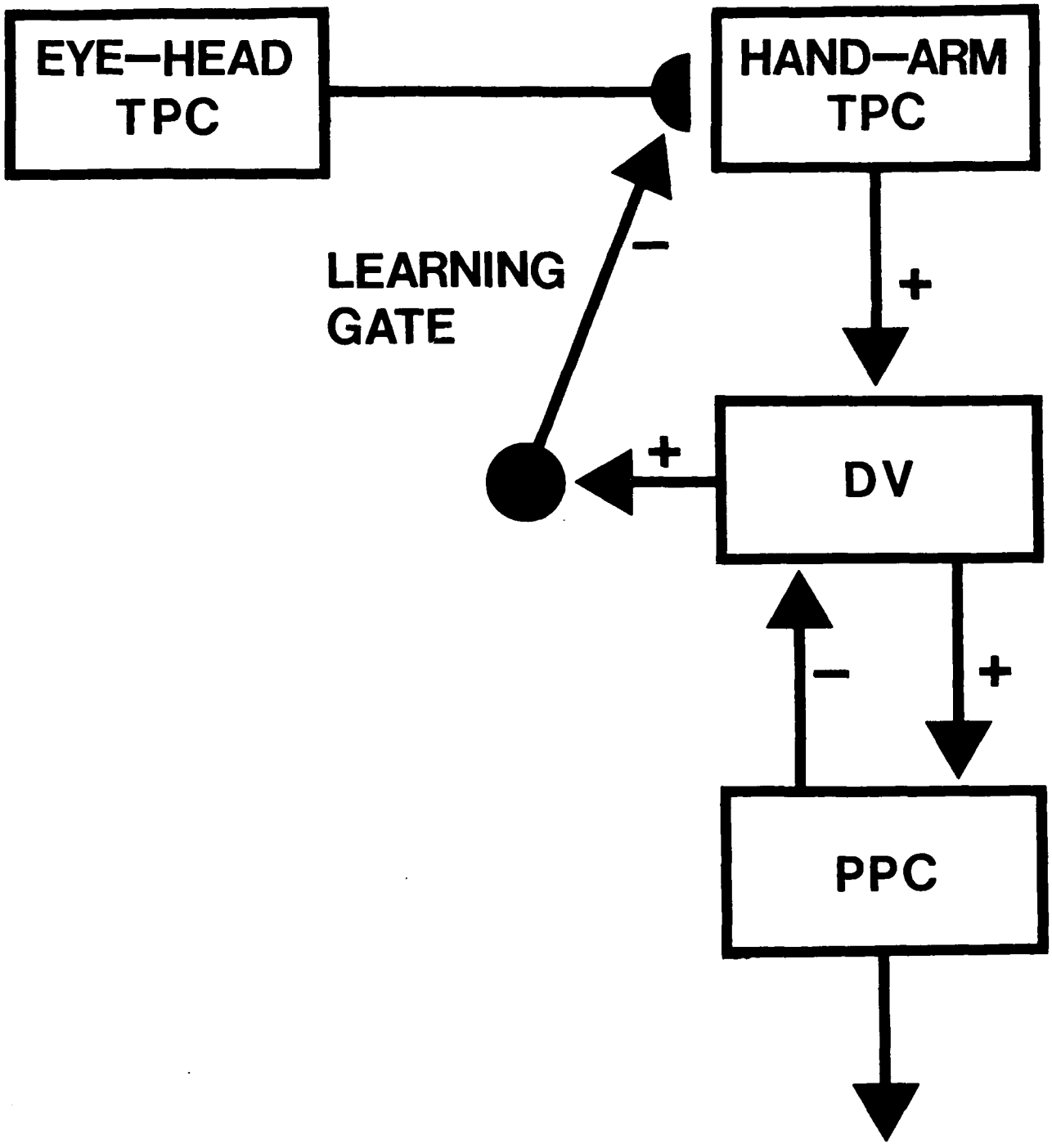

Figure 3

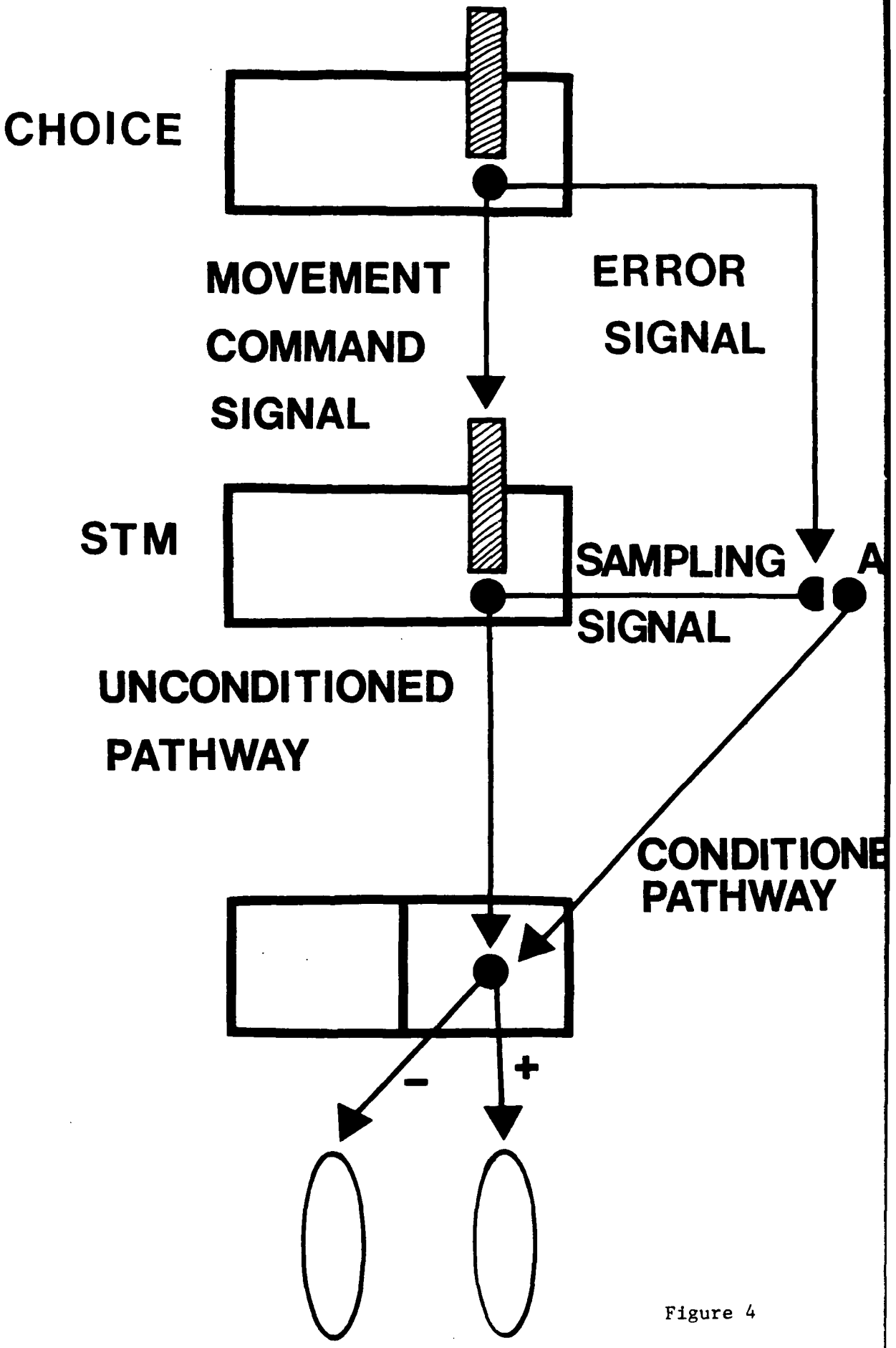
CHOICE
MOVEMENT
COMMAND
SIGNAL
ERROR
SIGNAL
STM
SAMPLING
SIGNAL
A
UNCONDITIONED
PATHWAY
CONDITIONE
PATHWAY
−
+

Figure 4

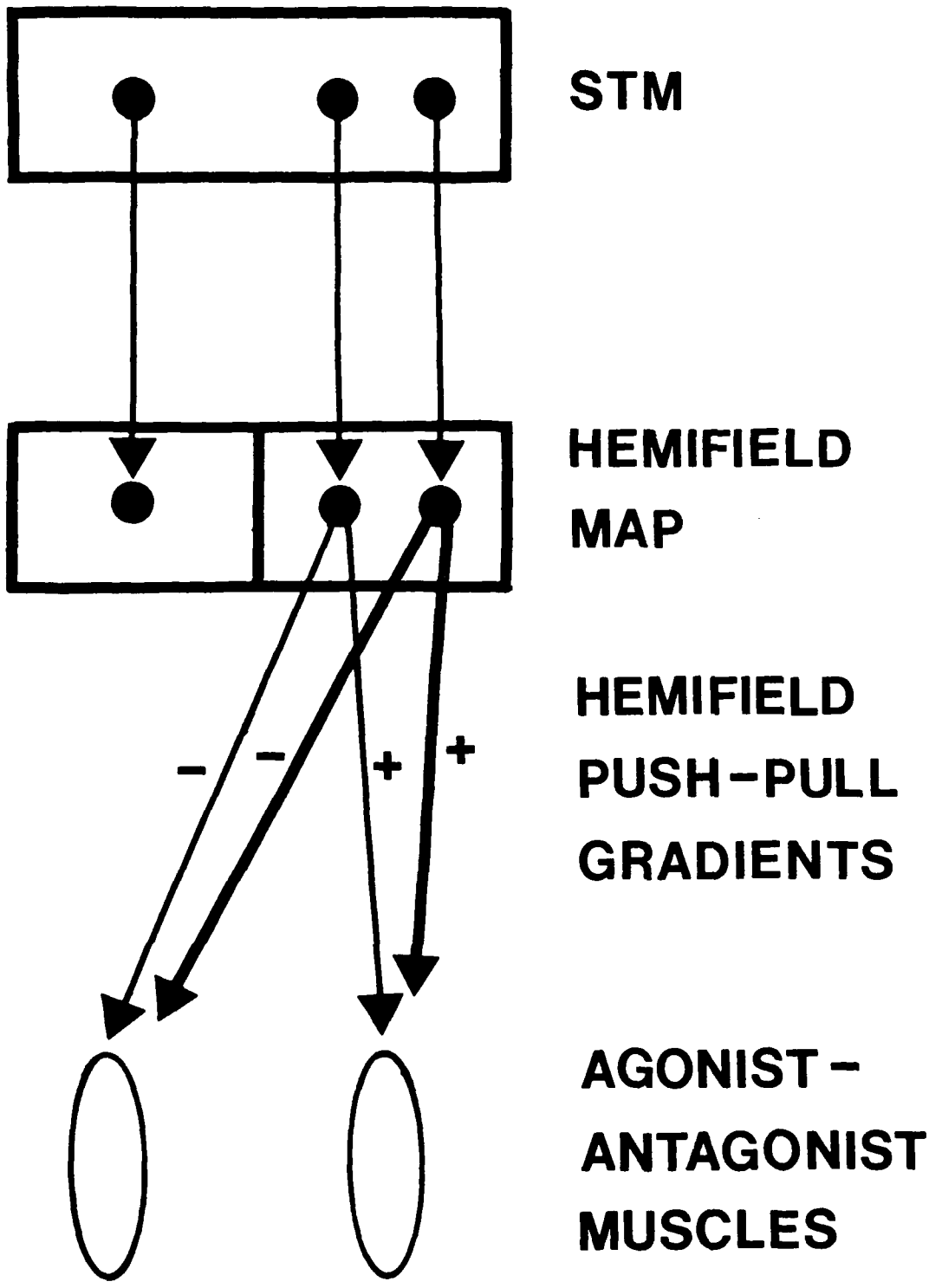
STM
HEMIFIELD MAP
HEMIFIELD PUSH-PULL GRADIENTS
AGONIST - ANTAGONIST MUSCLES
–
–
+
+

Figure 5

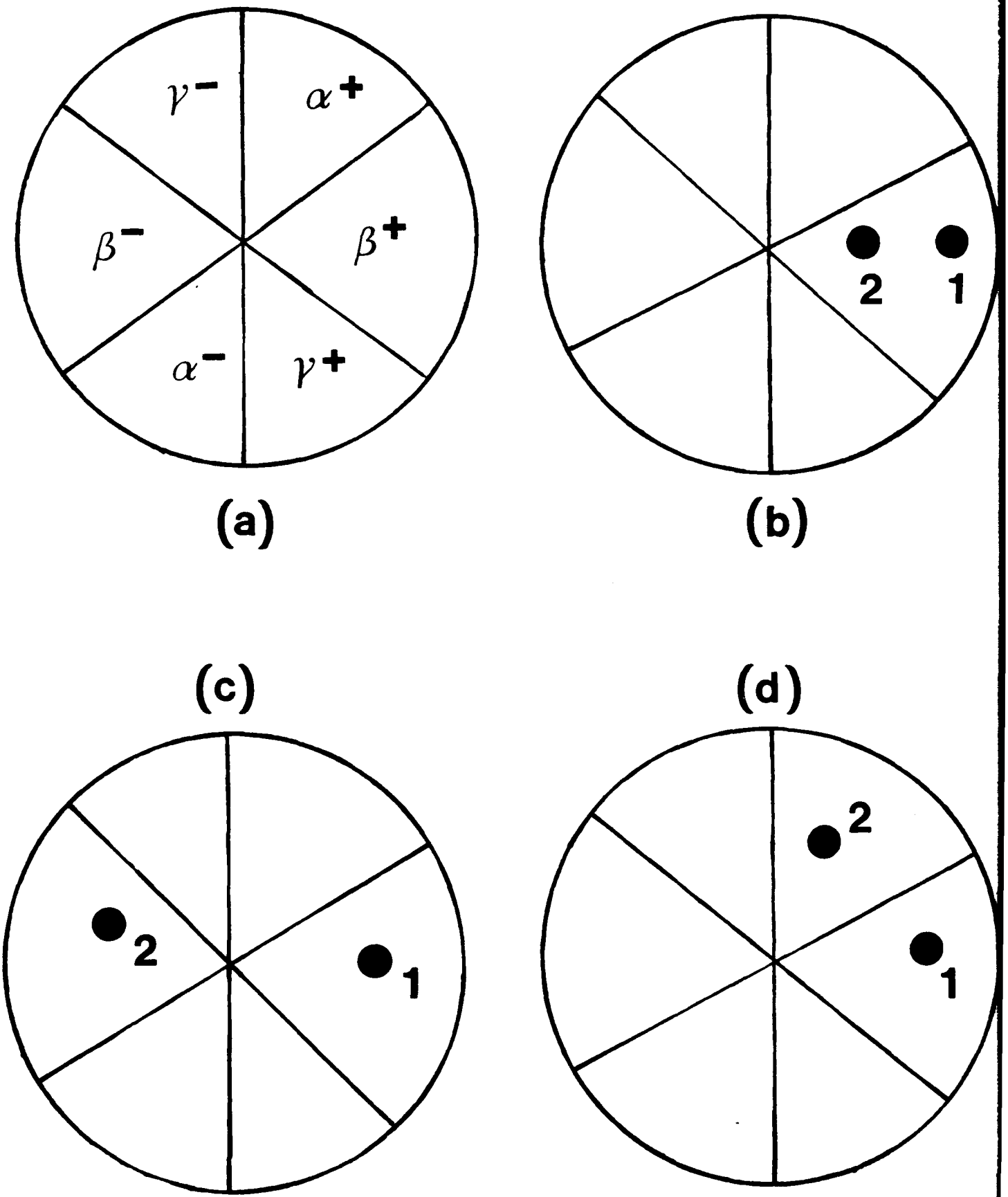

Figure 6

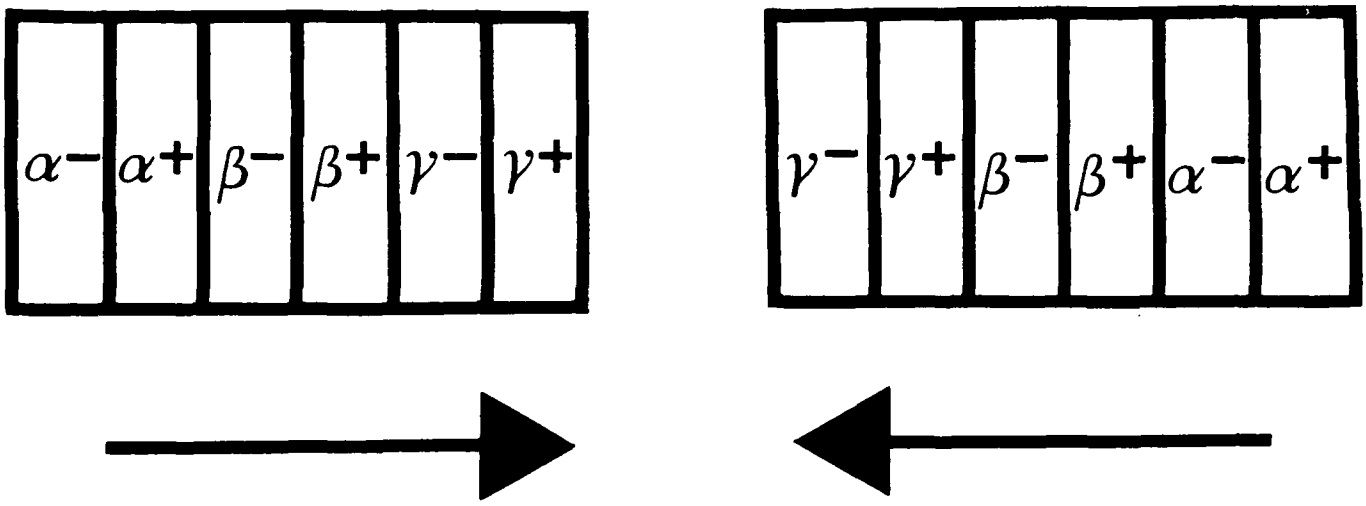

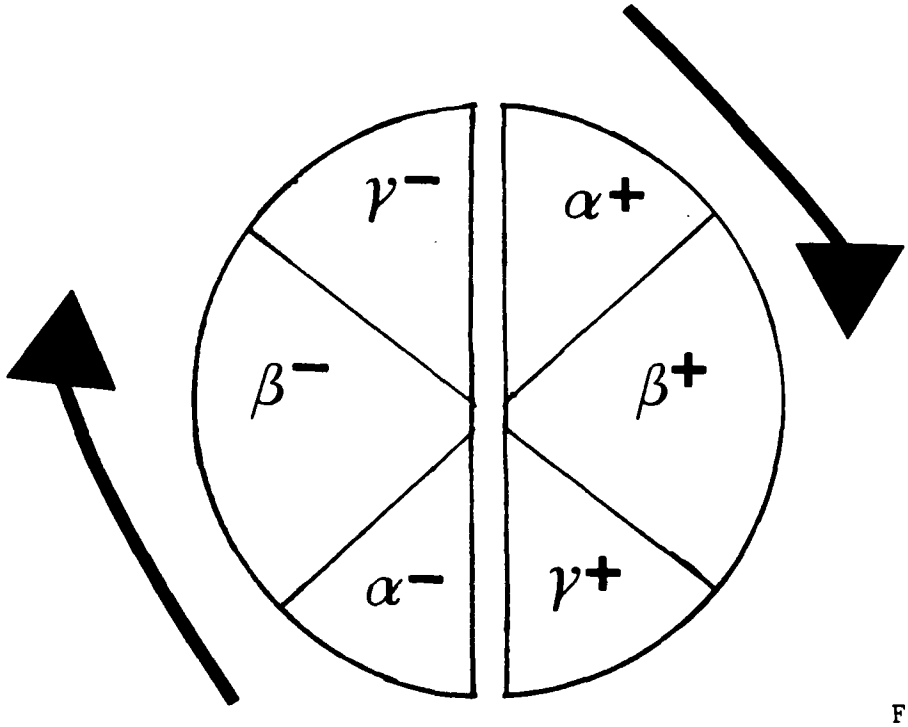

Figure 7

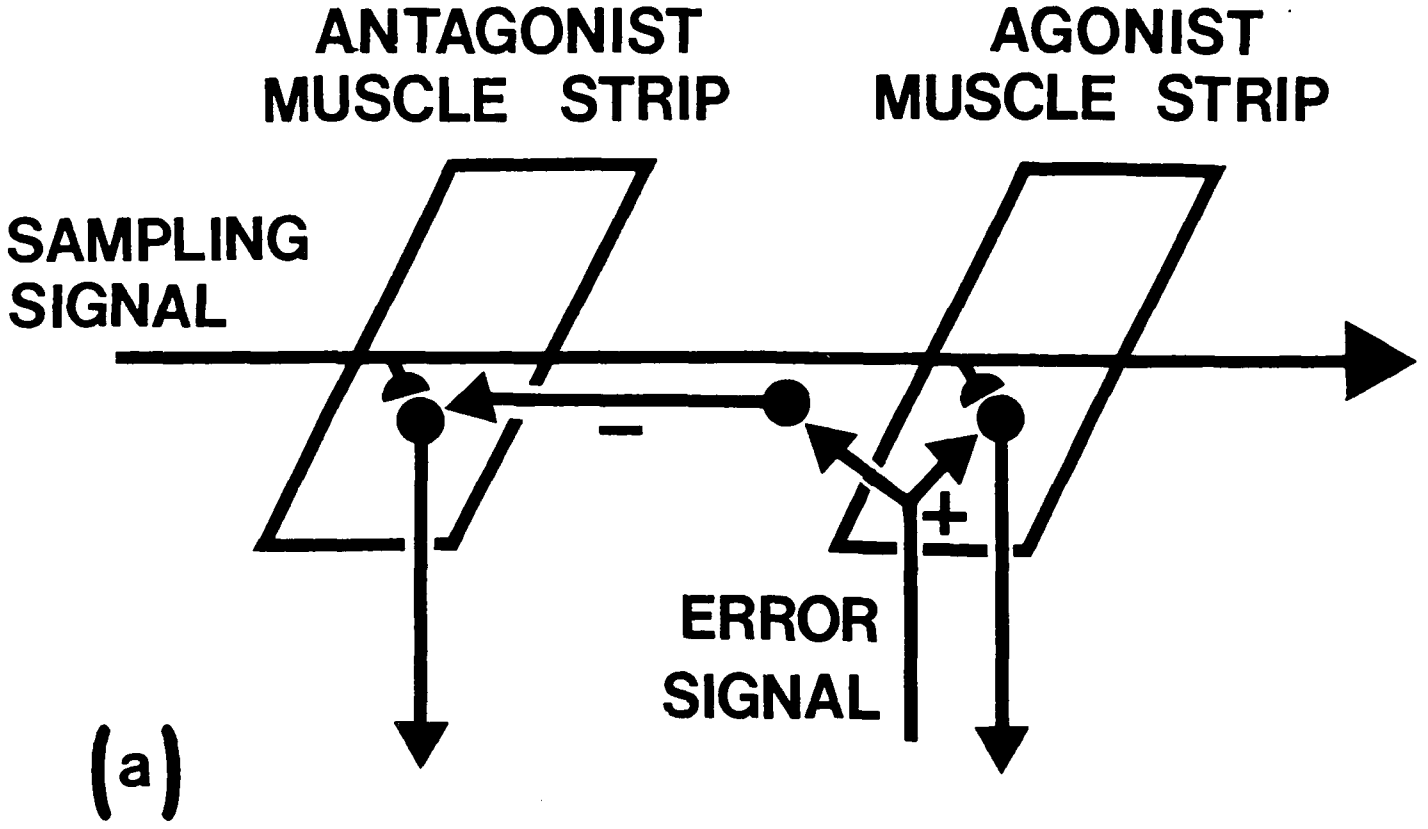
ANTAGONIST
MUSCLE STRIP
AGONIST
MUSCLE STRIP
SAMPLING
SIGNAL
−
+
−
ERROR
SIGNAL
(a)

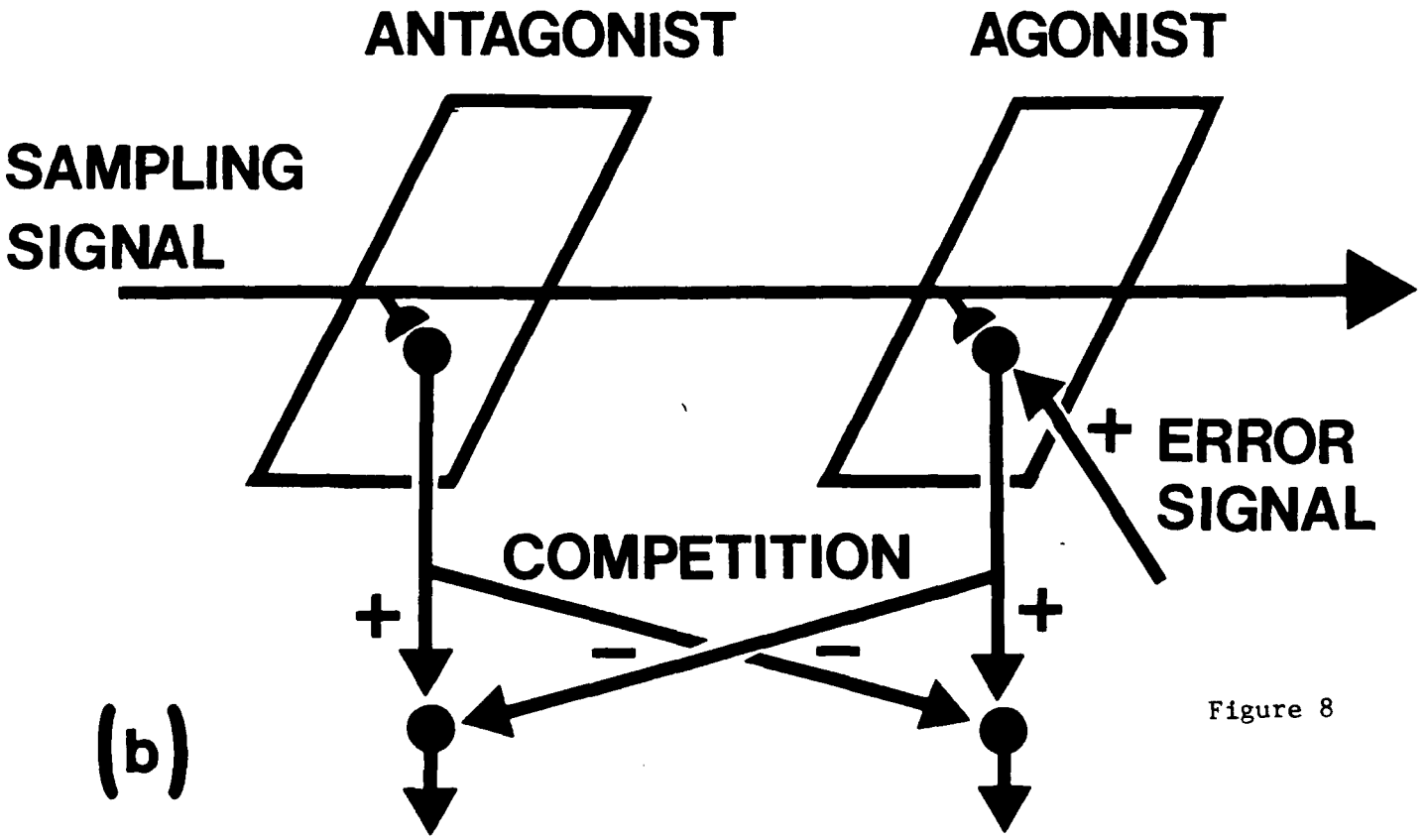
ANTAGONIST
AGONIST
SAMPLING
SIGNAL
+ ERROR
SIGNAL
COMPETITION
+
−
−
+
(b)

Figure 8